Since January 2020 Elsevier has created a COVID-19 resource centre with free information in English and Mandarin on the novel coronavirus COVID-19. The COVID-19 resource centre is hosted on Elsevier Connect, the company's public news and information website.

Microbial Pathogenesis 152 (2021) 104762

Contents lists available at ScienceDirect

Microbial Pathogenesis

journal homepage: www.elsevier.com/locate/micpath

Inhibitory efficiency of potential drugs against SARS-CoV-2 by blocking human angiotensin converting enzyme-2: Virtual screening and molecular dynamics study

Abdul Ashik Khan [a], Nabajyoti Baildya [b], Tanmoy Dutta [c], Narendra Nath Ghosh [a,*]

[a] Department of Chemistry, University of Gour Banga, Mokdumpur, Malda, 732103, India
[b] Department of Chemistry, University of Kalyani, Kalyani, 741235, India
[c] Departments of Chemistry, JIS College of Engineering, Kalyani, 741235, India

ARTICLE INFO

Keywords:
SARS-CoV-2
Molecular dynamics simulation
ACE-2
COVID-19
CPM

ABSTRACT

Till date millions of people are infected by SARS-CoV-2 throughout the world, while no potential therapeutics or vaccines are available to combat this deadly virus. Blocking of human angiotensin-converting enzyme 2 (ACE-2) receptor, the binding site of SARS-CoV-2 spike protein, an effective strategy to discover a drug for COVID-19. Herein we have selected 24 anti-bacterial and anti-viral drugs and made a comprehensive analysis by screened them virtually against ACE-2 receptor to find the best blocker by molecular docking and molecular dynamics studies. Analysis of results revealed that, Cefpiramide (CPM) showed the highest binding affinity of −9.1 kcal/mol. Furthermore, MD study for 10 ns and evaluation of parameters like RMSD, RMSF, radius of gyration, solvent accessible surface area analysis confirmed that CPM effectively binds and blocks ACE-2 receptor efficiently.

1. Introduction

The outbreak of COVID 19 caused by severe acute respiratory syndrome-related coronavirus (SARS-CoV-2) has thrown a pandemic threat to the humanity of the world [1]. Symptoms like cold, flu and in major cases lung failure or brain failure are shown by the infected patients [2]. This virus has a huge transmission rate, and without developing a suitable therapeutic option, the human lives can't come back in their previous rhythm [3].

Coronaviruses (CoVs) belong to the family of Coronaviride with spike glycoprotein on their outer surface, which is similar to severe acute respiratory syndrome (SARS) and middle east respiratory syndrome (MERS) [4]. SARS-CoV-2 is a large enveloped positive sense RNA virus containing structural and non-structural proteins (nsps), including several accessory proteins [5]. 82% genomic sequence identity of SARS-CoV-2 with SARS-CoV helps us to gather knowledge about the pathogenesis of SARS-CoV-2 [6]. SARS-CoV and SARS-CoV-2, S protein mediated host cell invasion occurred through binding angiotensin converting enzyme-2 (ACE-2), a receptor protein [6,7]. ACE-2 is located at the surface membrane of the host cell. The infection process initiates with the interaction between viral S protein and ACE-2 on the surface of the host cell [8]. According to the analysis of Cryo-EM structure, the binding affinity of S protein (SARS-CoV-2) with ACE-2 is approximately 10–20 times greater than the SARS-CoV S protein [9,10]. So higher contagiousness and transmissibility are reflected for SARS-CoV-2 with respect to SARS-CoV [11,12]. Various attempts have been made to inhibit different proteins and enzymes that are involved in replication process of SARS-CoV-2 viz. hydroxychloroquine inhibits Mpro [13], remdesivir inhibits RdRp [14], Sofosbuvir, Ribavirin inhibit RdRp [15], extract from Azadiractha Indica inhibits PL-pro [16]. Furthermore, to discover therapeutic agents for effective blocking of ACE-2 protein, Chloroquine and hydroxychloroquine are already reported [17,18,51].

Systematic checking of drug-drug target interaction (DTI) is a standard method of drug repurposing. Various scoring functions (e.g. docking scoring function) are applied for drug repurpose [17].

In this study, we have selected 24 anti-bacterial and anti-viral drugs for virtual screening against ACE2 proteins of human body. Molecular docking study has been done with ACE2 receptor against these drugs. Molecular dynamics simulation was also performed to check the stability of ACE2 with that drugs by different plots like RMSD, RMSF, SASA

* Corresponding author.
E-mail addresses: abdulashik0@gmail.com (A.A. Khan), nabajyotibaildya@gmail.com (N. Baildya), dutta.tanmoy88@gmail.com (T. Dutta), ghosh.naren13@gmail.com (N.N. Ghosh).

https://doi.org/10.1016/j.micpath.2021.104762
Received 16 July 2020; Received in revised form 15 October 2020; Accepted 24 January 2021
Available online 29 January 2021

Table 1
Docking score with resource of studied potentially active drugs.

Some potentially active drug for repurposing	Pubchem CID	MW (g/mol)	MF	Docking Score (Kcal/mol)	Ref
2-Amino-6-chloropurine	5360349	169.57	C5H4ClN5	−5.3	[26]
3-Pyridinemethanol	7510	109.13	C_6H_7NO	−4.5	[27]
Ametantrone	2134	412.5	$C_{22}H_{28}N_4O_4$	−7.0	[28]
Arfomoterol (Formoterol)	3083544	344.4	C19H24N2O4	−7.8	[29]
Arildone	41728	368.9	C20H29ClO4	−6.0	[30]
Azanidazole	6436171	246.23	C10H10N6O2	−5.9	[31]
Bometolol	68850	472.5	C25H32N2O7	−7.5	[32]
Cefpiramide	636405	612.6	C25H24N8O7S2	−9.1	[33]
Cletoquine	71826	307.82	C16H22ClN3O	−6.4	[34]
Denopamine	5311064	317.4	C18H23NO4	−6.4	[35]
Emiglitate	72004	355.4	C17H25NO7	−7.1	[36]
Flurocitabine	3034016	243.19	C9H10FN3O4	−6.5	[37]
Lasinavir	464372	659.8	C35H53N3O9	−7.8	[38]
Metossamina	688523	211.26	C11H17NO3	−5.7	[39]
Mitoxantrone	4212	444.5	C22H28N4O6	−7.2	[40]
Nifurpirinol	6436061	246.22	C12H10N2O4	−6.9	[41]
Oxiracetam	4626	158.16	C6H10N2O3	−5.1	[42]
Piroxantrone	59916	411.5	C21H25N5O4	−7.1	[43]
Stiripentol	5311454	234.29	C14H18O3	−6.4	[44]
Sulfinalol	44439	377.5	C20H27NO4S	−7.6	[45]
Teloxantrone	124644	411.5	C21H25N5O4	−7.1	[46]
Tigecycline	54686904	585.6	C29H39N5O8	−7.5	[47]
Toborinone	60790	384.4	C21H24N2O5	−7.6	[48]
Xamoterol	155774	339.39	C16H25N3O5	−6.5	[49]

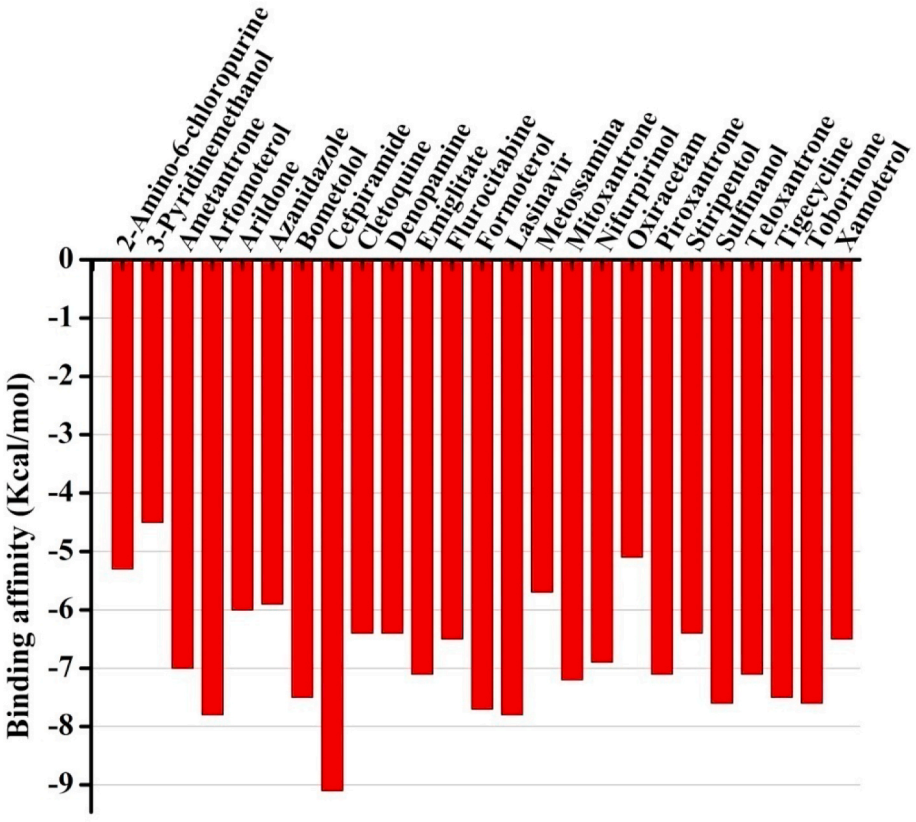

Fig. 1. Docking score of different compounds against ACE-2.

radius of gyration analysis.

2. Methodology

2.1. Molecular docking studies

The crystal structure of SARS-CoV-2 spike binding site angiotensin converting enzyme-2 (ACE-2) (PDB ID:6M0J) receptor was obtained from protein data bank (http://www.rcsb.org). The structure was then cleaned using Autodock tools by removing heteroatoms and by adding necessary hydrogen atoms. The structures of the 24 drug molecules were obtained from PubChem. Using UCSF Chimera [19] the pdb files of the drugs were created for docking. Only chain-A of ACE-2 receptor was selected for docking with drugs. Autodock Vina [20] package was used for docking between the best binding sites of ACE-2 and drugs.

Table 2
Toxicity prediction of compounds of ACE2 inhibitor.

Compound	AMES toxicity	Max. tolerated dose (human)	hERG I inhibitor	hERG II inhibitor	Oral Rat Acute Toxicity (LD50) (mol/kg)	Oral Rat Chronic Toxicity (LOAEL) (log mg/kg_bw/day)	Hepatot-oxicity	Skin Sensitis-ation	T.Pyriformis toxicity (log ug/L)	Minnow toxicity (log mM)
2-Amino-6-chloropurine	Yes	0.217	No	No	2.318	1.227	No	No	0.285	2.308
3-Pyridinemethanol	No	0.861	No	No	1.949	2.421	No	Yes	−0.684	2.307
Ametantrone	No	0.647	No	Yes	2.565	4.466	Yes	No	0.285	2.718
Arfomoterol (Formoterol)	No	0.144	No	Yes	2.725	2.666	Yes	No	0.348	1.198
Arildone	No	1.029	No	Yes	3.328	1.932	No	No	1.471	−1.579
Azanidazole	Yes	0.482	No	No	1.897	1.575	Yes	No	0.285	2.141
Bometolol	No	−0.106	No	Yes	2.019	1.757	Yes	No	0.327	−0.023
Cefpiramide	No	0.774	No	No	2.437	3.071	Yes	No	0.285	4.32
Cletoquine	No	0.436	No	Yes	2.717	1.371	Yes	No	0.672	2.641
Denopamine	No	−0.139	No	Yes	2.83	2.101	Yes	No	0.476	1.298
Emiglitate	No	0.927	No	No	2.215	3.652	Yes	No	0.284	4.156
Flurocitabine	No	1.08	No	No	2.491	2.357	No	No	0.311	3.591
Lasinavir	No	−0.242	No	Yes	2.535	2.631	Yes	No	0.285	−0.014
Metossamina	No	0.319	No	No	2.596	1.267	No	No	0.227	0.226
Mitoxantrone	No	0.689	No	Yes	2.499	2.605	Yes	No	0.285	5.057
Nifurpirinol	Yes	0.687	No	No	2.491	1.987	No	No	0.761	1.514
Oxiracetam	No	1.29	No	No	1.839	1.871	No	No	−0.52	3.878
Piroxantrone	No	0.76	No	Yes	2.479	3.902	Yes	No	0.285	3.195
Stiripentol	No	0.777	No	No	1.867	1.965	No	No	2.045	0.612
Sulfinalol	No	0.262	No	Yes	2.69	2.106	Yes	No	0.403	0.184
Teloxantrone	Yes	0.647	No	Yes	2.483	3.489	Yes	No	0.285	4.036
Tigecycline	No	0.622	No	Yes	2.274	3.327	No	No	0.285	5.424
Toborinone	No	−0.294	No	Yes	2.883	1.297	Yes	No	0.308	1.311
Xamoterol	No	−0.235	No	No	1.536	1.239	Yes	No	0.27	5.022

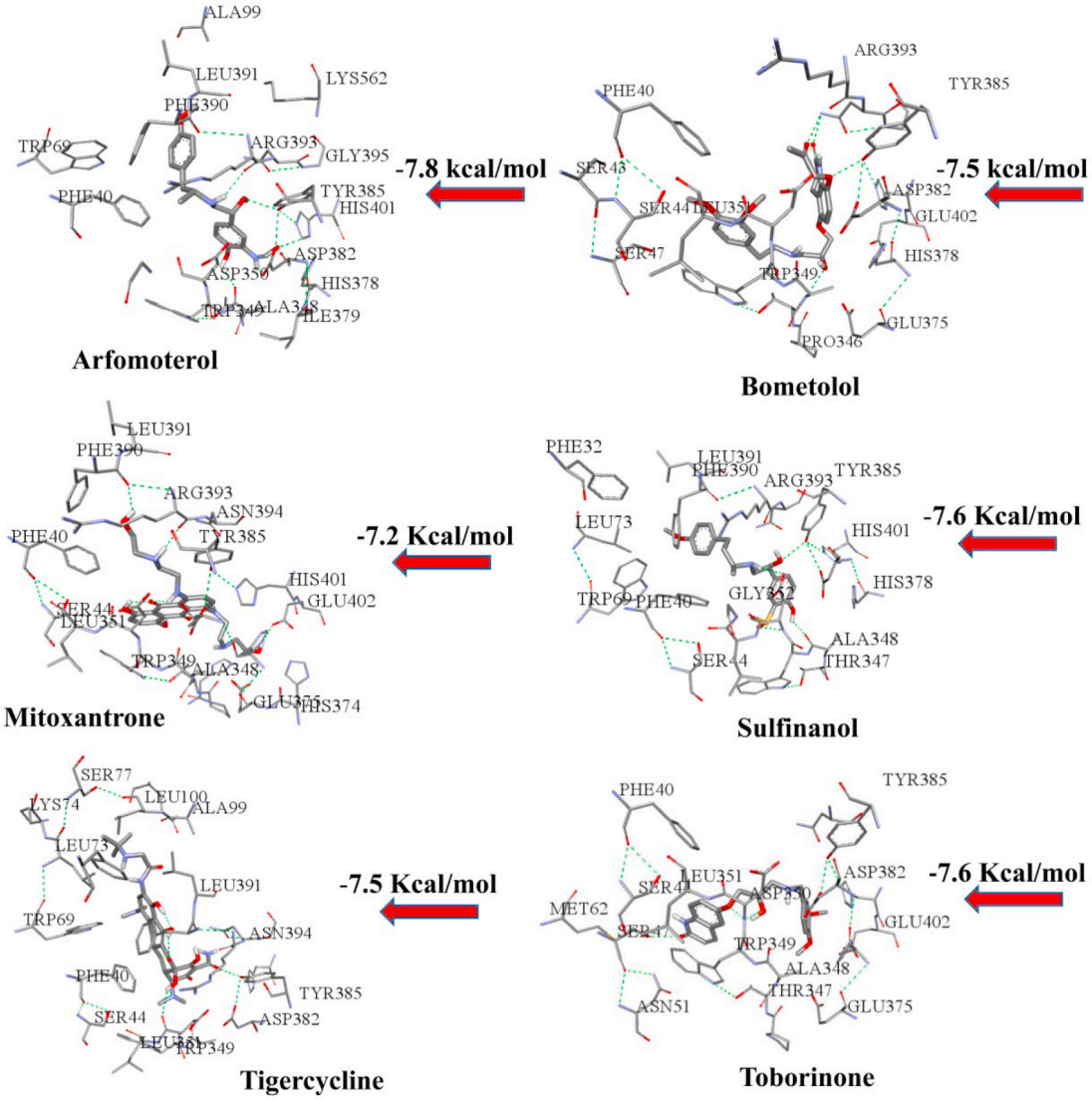

Fig. 2. Docked structure of ACE2 receptor with few drugs having high binding affinity.

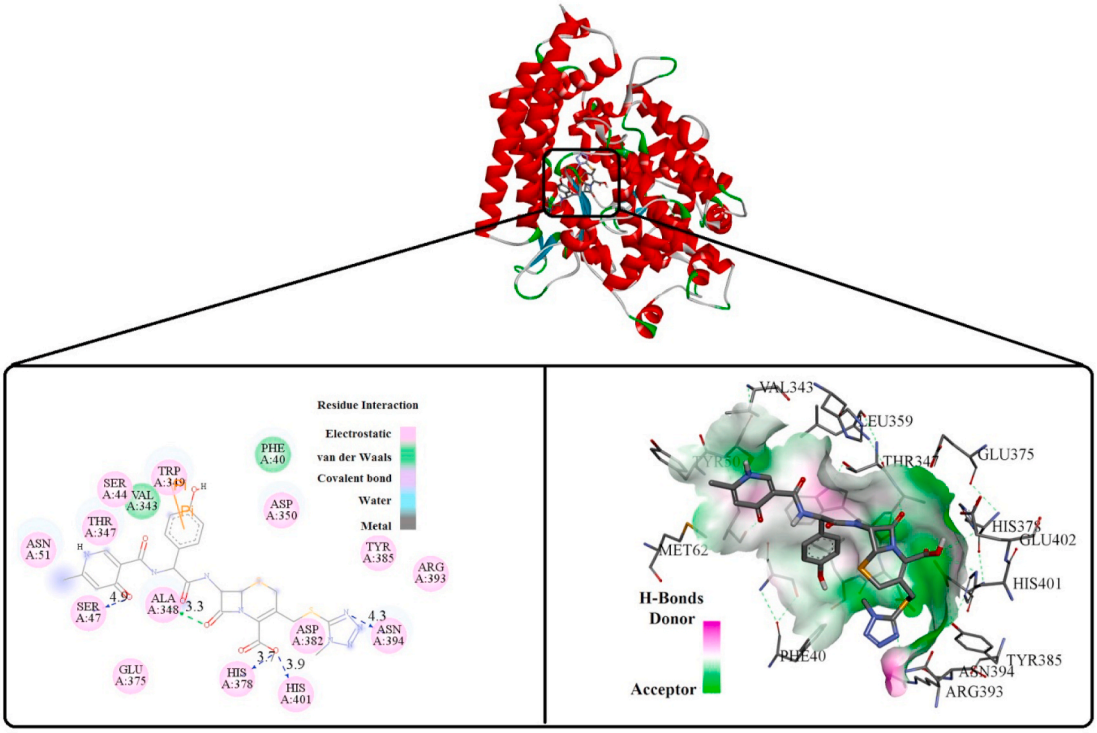

Fig. 3. Docked structure of Cefpiramide (CPM) docked ACE2.

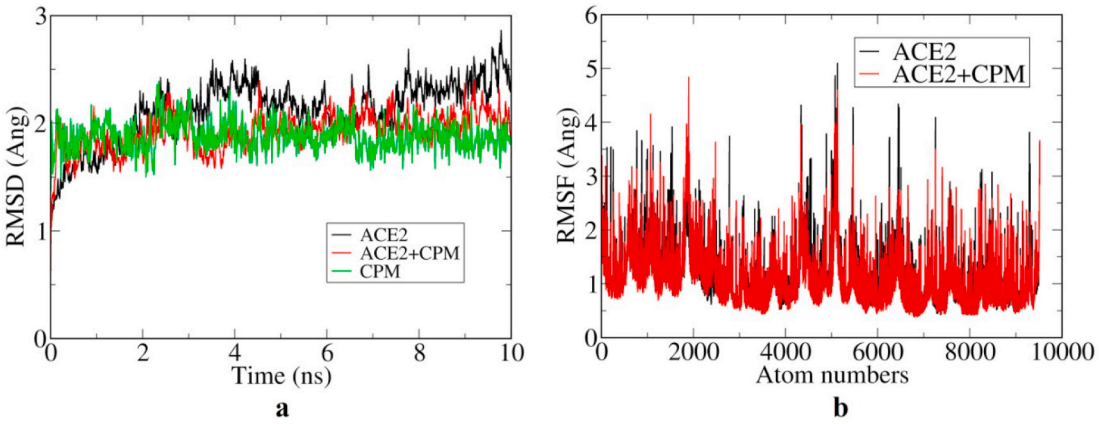

Fig. 4. RMSD plot (a) and RMSF plot for undocked and docked ACE2.

2.2. Molecular dynamics (MD) simulation studies

10ns MD-simulation was performed with the minimum energy conformer of the ACE-2 and Cefpiramide (CPM) complex using Gromacs (5.1) [20] with CHARMM36-march2019 force field [21]. The TIP3P water model [22] was used for solvation of the complex. Necessary topology and parameter files for the drug (CPM) were generated by using CGenFF server. A cubical box with a buffer dimension $10 \times 10 \times 10$ Å^3 was created and adequate number of Na^+ ions were added to maintain electro neutrality. After performing energy minimization of the ACE-2-drug complex to 10 kJ mol^{-1}nm^{-1}, a 100 ps NVT equilibration was then performed at 300 K followed by another equilibration NPT for 100 ps, keeping 2fs time step.

Modified Berendsen thermostat was used for the NPT ensemble. Here also the time step was 2 fs? For both NVT and NPT equilibration, cut-offs for electrostatic and van der Waals interactions were kept at 1.0 nm. Long range interactions were calculated using smooth particle mesh Ewald (PME) method [23]. The equilibrated ensembles were finally subjected to MD simulation for 10 ns, with electrostatic and van der Waals cut off as before. PME method was used to calculate long range electrostatic interactions. A modified Berendsen thermostat and a Parinello-Rahman barostat were used with reference temperature and pressure at 300 K and 1 bar respectively. Snapshots of the trajectory were saved every 1 ns for each case.

2.3. Binding free energy calculation

Molecular mechanics Poison-Boltzmann surface area (MM-PBSA) method [24], implemented on Gromacs tool (g_mmpbsa) [25] was used for the calculation of binding free energies. The binding energies were calculated by using the following formulae

$$\Delta G_{bind} = G_{w\text{-}complex} - G_{w\text{-}protein} - G_{w\text{-}drug} \quad (1)$$

$$G_{w\text{-}complex} = \langle E_{MM} \rangle + \langle G_{sol} \rangle - TS \quad (2)$$

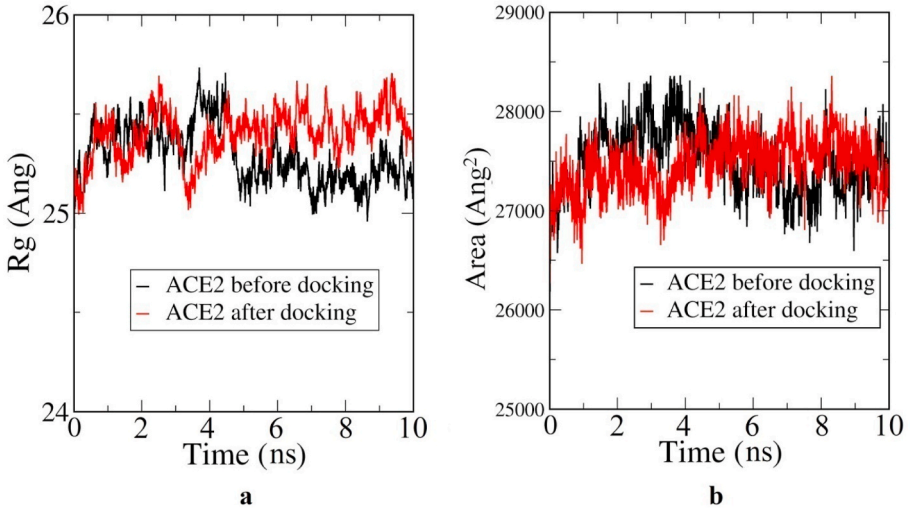

Fig. 5. Radius of gyration plot (a) and SASA plot (b) of undocked and CPM docked ACE-2.

Fig. 6. Structural alteration of amino acid in undocked and docked ACE-2.

$$E_{MM} = E_{bonded} + E_{non\text{-}bonded} = E_{bonded} + (E_{vdW} + E_{elec}) \quad (3)$$

$$G_{sol} = G_{polar} + G_{non\text{-}polar} = G_{polar} + (\gamma SASA + b) \quad (4)$$

Where, $G_{w\text{-}complex}$ is the total free energy of the ACE2 and drug complex, $G_{w\text{-}protein}$, $G_{w\text{-}drug}$ are the free energies of the protein and drug respectively. E_{MM} is the average MM potential energy including bonding, non-bonding energies, G_{sol} is the free energy of solvation including polar and non-polar energies. SASA is the solvent accessible surface area, γ is the coefficient of surface tension of solvent and b is the fitting parameter. TS is not considered by g_mmpbsa.

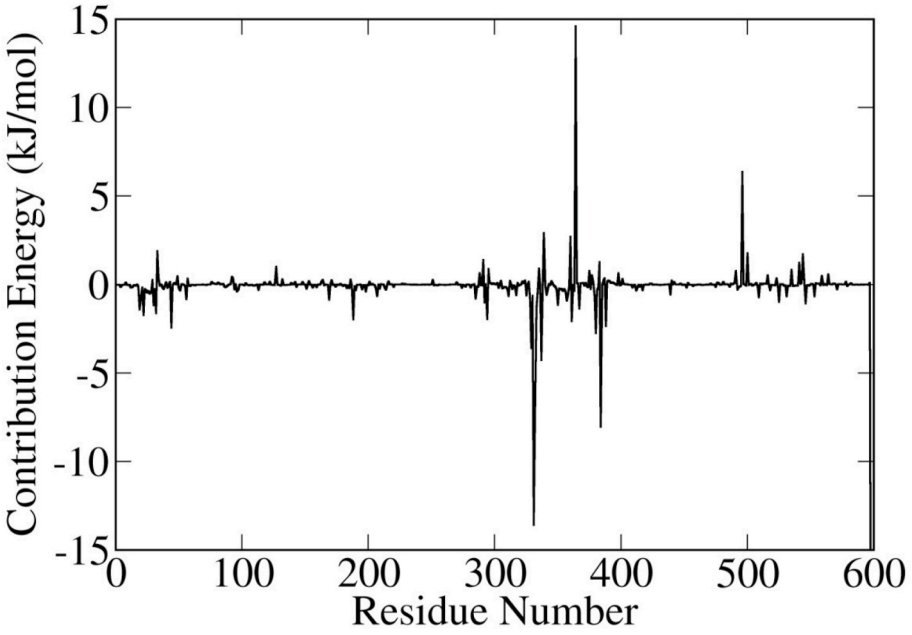

Fig. 7. Contribution of residues to binding energy in the docked structure of ACE2.

Table 3
Different types of interaction energies between ACE2 and CPM.

System	Binding Energy (kJ/mol)	van der Waal energy (kJ/mol)	Electrostatic energy (kJ/mol)	Polar solvation energy (kJ/mol)	SASA energy (kJ/mol)
ACE2+CPM	−79.958 ± 18.653	−172.786 ± 15.261	−59.125 ± 15.418	170.592 ± 24.815	−18.638 ± 1.223

3. Results and discussions

24 potentially active drugs were selected for virtual screening against human angiotensin converting enzyme-2 (ACE-2) receptor. According to the previous studies, all these drugs have either anti-bacterial or anti-viral activities as shown in Table 1. Among the selected drugs four drugs (Formoterol, Cefpiramide, Mitoxantrone and Tigecycline) are FDA approved. In the present study we have made a comprehensive analysis of the inhibitory activity of these drugs against ACE-2 receptor. Docking scores, summarised in Table 1 clearly indicate the binding efficiency of these drugs with ACE-2 receptor. All the 24 drugs showed binding affinities with ACE-2 receptor and 12 of them showed high binding affinities with a docking score greater than or equals to −7.0 kcal/mol.

Cefpiramide, which showed a broad spectrum antibiotic activity showed the highest docking score against the human ACE-2 receptor of −9.1 kcal/mol. The binding affinities of the studied drugs against ACE-2 are shown in Fig. 1.

Pharmacological analysis of these compounds showed interesting results. ADME toxicity analysis has been performed against these selected compounds.

3.1. ADMET calculations

ADMET (i.e. Absorption, Distribution, Metabolism, Excretion, and Toxicity) profiling of the compounds were performed with the help of pkCSM online server [50]. All the studied compounds have skin permeability ranging from −2.665 to −4.3. Most of the compounds do not inhibit P-glycoprotein I and II. Blood-brain barrier (BBB) permeability values are between −2.083 and +0.087, whereas CNS permeability values appear between −5.4 and −1.632. Most of the drugs do not inhibit CYP1A2, CYP2C19, CYP2C9, CYP2D6, CYP3A4 enzymes and do not interact with renal OCT2 substrate. Along with that, most of the drugs neither show AMES toxicity nor inhibit the hERGI inhibitor. The highest value of LD50 toxicity of these drugs are 3.328 mol/kg. Few of them are hepatotoxic in nature and almost all of them do not create skin sensitization. The highest value of minnow toxicity level of these drugs is 5.424. These values are tabulated in Table 2.

Compounds which showed potential binding affinities with ACE2 are shown in Fig. 2. The interaction site of the docked structure of the drugs with ACE2 is given in the figure.

Fig. 3 represents the docked structure of Cefpiramide (CPM) with ACE2. From Fig. 3 it is clear that there is strong binding interaction between the drug and ACE2 receptor due to the formation of H-bonding, electrostatic and van der Waal interactions. The nearest residues are shown in the 2D contour plot (left panel) as well as in the 3D structure is shown in right panel. The H-bonding distances (in angstrom) are given in the 2D structure and the donor and acceptor sites within the docked cavity are given in the right panel 3D structure.

Analysing the ADME data and binding energies obtained from docking results we have chosen the drug Cefpiramide (CPM BE = −9.1 kcal/mol) to study the MD-simulation against ACE-2. The RMSD plot of the docked CPM against ACE-2 is shown in Fig. 4. We found a profound stabilization of the docked structure after 2 ns?as compared to the undocked one.

Furthermore, we also note that after 2 ns the RMSD fluctuation of the docked structure is relatively low with respect to the undocked one suggesting during the progress of MD-simulation, the drug moiety interacts strongly within the cavity of the ACE-2. RMSF plot as shown in Fig. 4b reveals that the fluctuations of residues for the docked structure are quite low compared to the undocked one. Radius of gyration (Rg) indicates the compactness of a system. With increasing the value of Rg, the compactness of the system also increases. Rg for the docked and undocked structure is shown in Fig. 5a. Rg for the docked structure is quite high as compared to the undocked one which confirms that after docking the drug (CPM) is nicely fitted within the cavity of ACE-2. We

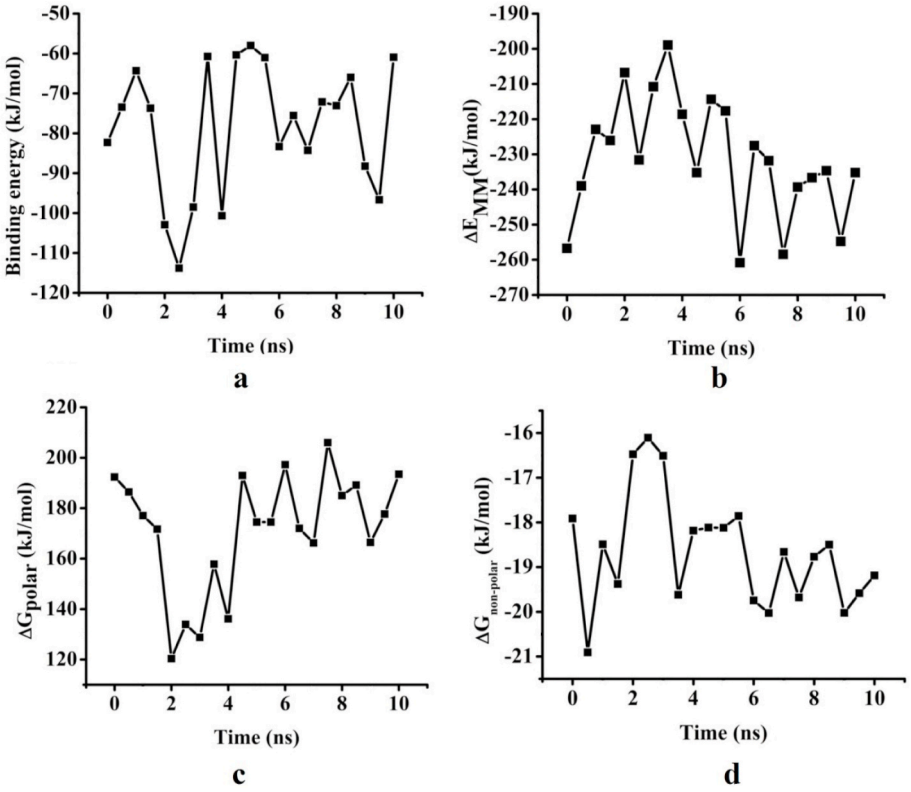

Fig. 8. Variation of different binding energy components: (a) Binding energy, (b)ΔE_{MM}, (c) ΔG_{polar} and (d) $\Delta G_{non\text{-}polar}$ with time.

also analyzed the surface accessible surface area (SASA) plot for undocked and docked ACE-2.

Fig. 5b represents the SASA plot of undocked and docked ACE-2. A closer look to Fig. 5b revealed that after 4 ns the docked structure corresponds to the higher SASA value compared to the undocked one suggesting the entry of the drug stabilizes ACE-2 conformation. Fig. 6 represents the sequence analysis of undocked and docked ACE-2. From Fig. 6 it is clear that there is a substantial structural alternation on amino acids in ACE2 before and after docking. Residue numbers from 280 to 381 of ACE2 were mostly affected by the drug CPM. This result is further elevated by the contribution energy with respect to residue number, as shown in Fig. 7.

The binding energy of CPM against ACE2 showed a high value of -79.958 ± 18.653 kJ/mol. As shown in Table 3 all the interaction energies between ACE2 and CPM showed a high value confirming profound conformational changes of ACE2 by CPM.

Fig. 8 represents the binding free energy, MM energy, polar solvation and non-polar solvation energy. The binding free energy of polar and non-polar parts of the docked structure with respect to time is shown in Fig. 8 c & d respectively. During MD-simulation non-polar binding free energy (van der Waal interaction) decreased indicating much stronger binding of the drug CPM in the ACE2 cavity. A stronger binding between CPM and ACE2 is indicated by the substantial structural change in ACE2 receptor. Fig. 8 a & b represented the binding energy and MM energy of CPM against ACE2 during MD-simulation. We found the average binding energy of −79.958 kJ/mol and the average MM energy of −231.327 kJ/mol.

Conformational changes during MD-simulation is represented in Fig. 9. These changes are captured at each nanosecond and revealed that these changes are profound. RMSD plot indicates a significant change in the structure after two ns. Hence it is clear that CPM has a considerable impact on the conformation of ACE-2.

4. Conclusion

In the present work, we have virtually screened 24 potentially active anti-bacterial and anti-viral drugs against SARS-CoV-2 binding receptor, ACE-2. ADMET profiling confirms that these drugs are suitable to use against COVID-19 treatment. The screening results revealed that cefpiramide (CPM) showed a decent binding affinity SARS-CoV-2 human ACE-2 receptor. CPM entry to the cavity of ACE-2 is facilitated by forming H-bonding interactions and electrostatic interactions. Furthermore, MD-simulation of CPM against ACE-2 showed a striking result by stabilizing ACE-2 conformation. The total disruption of ACE-2 sequence indicates that the drug has a significant impact on the receptor. Considerable stabilization and effective blocking of ACE-2 by CPM are confirmed by RMSD, RMSF analysis along with the binding energy calculation. We believe that the drug, CPM can be anticipated as an effective blocker for ACE-2 receptor and showed potential inhibitory activity against SARS-CoV-2.

Data availability

Data is available upon request to the corresponding author.

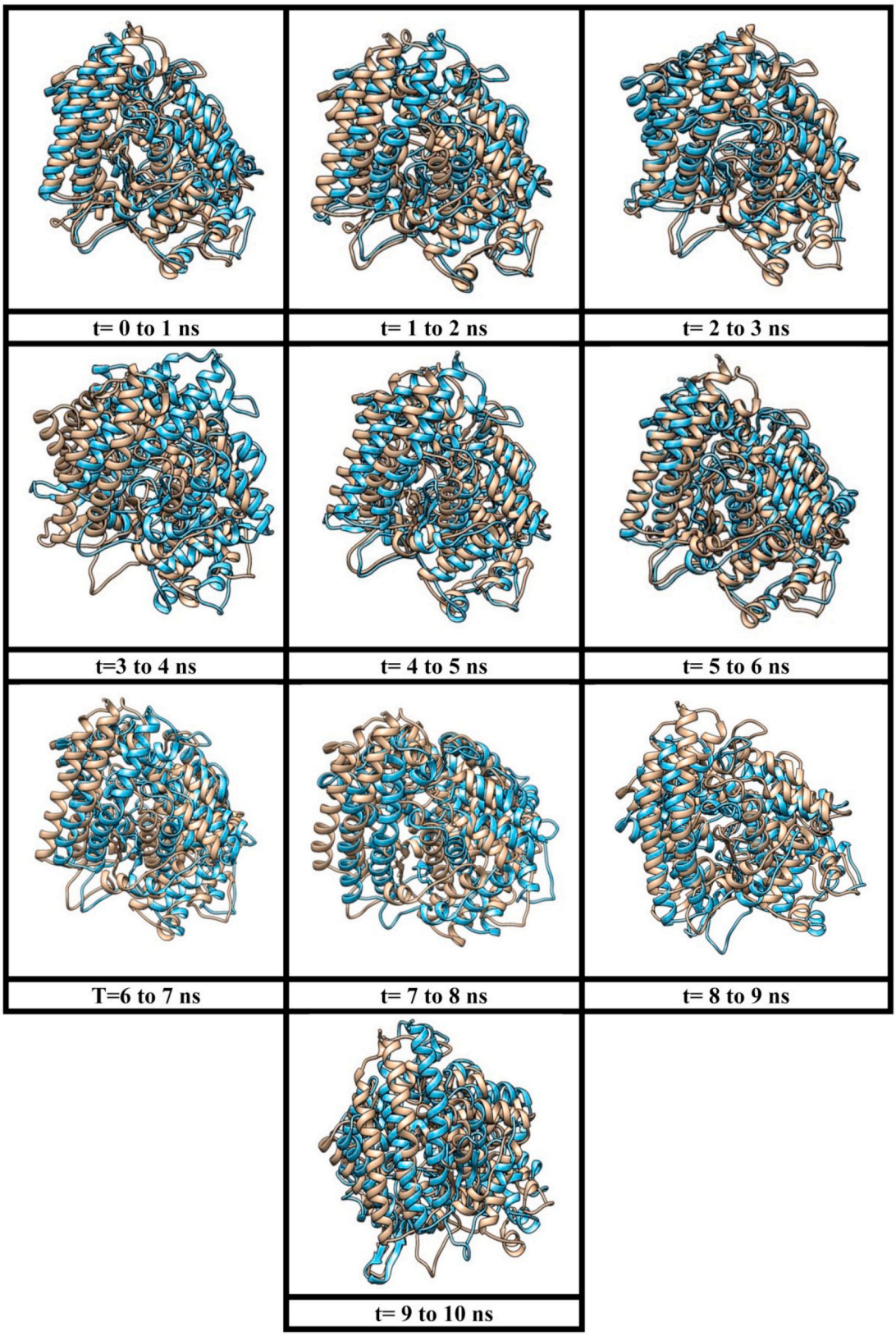

Fig. 9. Conformational changes of the docked structure of ACE2 at each nanosecond during MD-simulation [t = (n-1)ns, brown and t = n ns, sky-blue; n = 0–10 ns]

Declaration of competing interest

The authors declare no conflicting interest in the present work.

References

[1] X. Xu, P. Chen, J. Wang, J. Feng, H. Zhou, X. Li, et al., Evolution of the novel coronavirus from the ongoing Wuhan outbreak and modeling of its spike protein for risk of human transmission, Sci. China Life Sci. 63 (2020) 457–460.

[2] V. Jain, J.-M. Yuan, Predictive symptoms and comorbidities for severe COVID-19 and intensive care unit admission: a systematic review and meta-analysis, International Journal of Public Health (2020) 1.

[3] M. Jayaweera, H. Perera, B. Gunawardana, J. Manatunge, Transmission of COVID-19 virus by droplets and aerosols: a critical review on the unresolved dichotomy, Environ. Res. (2020) 109819.

[4] S. Su, G. Wong, W. Shi, J. Liu, A.C. Lai, J. Zhou, et al., Epidemiology, genetic recombination, and pathogenesis of coronaviruses, Trends Microbiol. 24 (2016) 490–502.

[5] Y. Indwiani Astuti, Severe acute respiratory syndrome coronavirus 2 (SARS-CoV-2): an overview of viral structure and host response. Diabetes & metabolic syndrome, 2020.

[6] W. Liu, J.S. Morse, T. Lalonde, S. Xu, Learning from the past: possible urgent prevention and treatment options for severe acute respiratory infections caused by 2019-nCoV, Chembiochem 21 (5) (2020) 730–738.

[7] J.F.-W. Chan, K.-H. Kok, Z. Zhu, H. Chu, K.K.-W. To, S. Yuan, et al., Genomic characterization of the 2019 novel human-pathogenic coronavirus isolated from a patient with atypical pneumonia after visiting Wuhan, Emerg. Microb. Infect. 9 (2020) 221–236.

[8] H. Hofmann, S. Pöhlmann, Cellular entry of the SARS coronavirus, Trends Microbiol. 12 (2004) 466–472.

[9] R. Lu, X. Zhao, J. Li, P. Niu, B. Yang, H. Wu, et al., Genomic characterisation and epidemiology of 2019 novel coronavirus: implications for virus origins and receptor binding, Lancet 395 (2020) 565–574.

[10] D. Wrapp, N. Wang, K.S. Corbett, J.A. Goldsmith, C.-L. Hsieh, O. Abiona, et al., Cryo-EM structure of the 2019-nCoV spike in the prefusion conformation, Science 367 (2020) 1260–1263.

[11] B. Tang, N.L. Bragazzi, Q. Li, S. Tang, Y. Xiao, J. Wu, An updated estimation of the risk of transmission of the novel coronavirus (2019-nCov), Infectious disease modelling 5 (2020) 248–255.

[12] R. Li, S. Pei, B. Chen, Substantial undocumented infection facilitates the rapid dissemination of novel coronavirus (SARS-CoV2), 2020 published online ahead of print March 16.

[13] N. Baildya, N.N. Ghosh, A.P. Chattopadhyay, Inhibitory activity of hydroxychloroquine on COVID-19 main protease: an insight from MD-simulation studies, J. Mol. Struct. (2020) 128595.

[14] E.P. Tchesnokov, J.Y. Feng, D.P. Porter, M.J.V. Götte, Mechanism of inhibition of Ebola virus RNA-dependent RNA polymerase by remdesivir 11 (2019) 326.

[15] A.A. Elfiky, Anti-HCV, nucleotide inhibitors, repurposing against COVID-19, Life Sci. (2020) 117477.

[16] N. Baildya, A.A. Khan, N.N. Ghosh, T. Dutta, A.P. Chattopadhyay, Screening of potential drug from Azadiractha Indica (Neem) extracts for SARS-CoV-2: an insight from molecular docking and MD-simulation studies, J. Mol. Struct. (2020) 129390.

[17] J. Fantini, C. Di Scala, H. Chahinian, N. Yahi, Structural and molecular modeling studies reveal a new mechanism of action of chloroquine and hydroxychloroquine against SARS-CoV-2 infection, Int. J. Antimicrob. Agents (2020) 105960.

[18] R.L. Kruse, Therapeutic strategies in an outbreak scenario to treat the novel coronavirus originating in Wuhan, China, F1000Research (2020) 9.

[19] E.F. Pettersen, T.D. Goddard, C.C. Huang, G.S. Couch, D.M. Greenblatt, E.C. Meng, et al., UCSF Chimera—a visualization system for exploratory research and analysis, J. Comput. Chem. 25 (2004) 1605–1612.

[20] O. Trott, A.J. Olson, AutoDock Vina: improving the speed and accuracy of docking with a new scoring function, efficient optimization, and multithreading, J. Comput. Chem. 31 (2010) 455–461.

[21] S. Lee, A. Tran, M. Allsopp, J.B. Lim, Hénin Jrm, Klauda JB. CHARMM36 united atom chain model for lipids and surfactants, J. Phys. Chem. B 118 (2014) 547–556.

[22] S. Boonstra, P.R. Onck, E. van der Giessen, CHARMM TIP3P water model suppresses peptide folding by solvating the unfolded state, J. Phys. Chem. B 120 (2016) 3692–3698.

[23] M.J. Abraham, J.E. Gready, Optimization of parameters for molecular dynamics simulation using smooth particle-mesh Ewald in GROMACS 4.5, J. Comput. Chem. 32 (2011) 2031–2040.

[24] R. Kumari, R. Kumar, , Consortium OSDD, A. Lynn, g_mmpbsa A GROMACS tool for high-throughput MM-PBSA calculations, J. Chem. Inf. Model. 54 (2014) 1951–1962.

[25] N.A. Baker, D. Sept, S. Joseph, M.J. Holst, J.A. McCammon, Electrostatics of nanosystems: application to microtubules and the ribosome, Proc. Natl. Acad. Sci. Unit. States Am. 98 (2001) 10037–10041.

[26] V. Krasnov, A.Y. Vigorov, D. Gruzdev, G. Levit, M. Kravchenko, S. Skornyakov, et al., Tuberculostatic activity of 2-amino-6-chloropurine derivatives, Pharmaceut. Chem. J. 51 (2017) 769–772.

[27] S. Durdagi, B. Aksoydan, B. Dogan, K. Sahin, A. Shahraki, N. Birgül-İyison, Screening of clinically approved and investigation drugs as potential inhibitors of SARS-CoV-2 main protease and spike receptor-binding domain bound with ACE2 COVID19 target proteins: a virtual drug repurposing study, 2020.

[28] M. Piccart, M. Rozencweig, R. Abele, E. Cumps, P. Dodion, D. Dupont, et al., Phase I clinical trial with ametantrone (NSC-287513), Eur. J. Cancer Clin. Oncol. 17 (1981) 775–779.

[29] C.R. Jenkins, E.D. Bateman, M.R. Sears, P.M. O'Byrne, What have we learnt about asthma control from trials of budesonide/formoterol as maintenance and reliever? Respirology, 2020.

[30] K. Kim, V. Sapienza, R. Carp, Antiviral activity of arildone on deoxyribonucleic acid and ribonucleic acid viruses, Antimicrob. Agents Chemother. 18 (1980) 276–280.

[31] M. Marchionni, A. Degli Innocenti, C. Penna, Combined systemic and topical treatment of trichomoniasis vaginalis with azanidazol, Clin. Exp. Obstet. Gynecol. 8 (1981) 18–20.

[32] T. Watanabe, Y. Watanabe, Y. Hasegawa, Y. Kudo, K. Kawashima, H. Sokabe, Acute and subchronic effects of bometolol on blood pressure in hypertensive rats, J. Pharmacobio-Dyn 4 (1981) 505–512.

[33] H. Wang, Y. Yu, X. Xie, C. Wang, Y. Zhang, Y. Yuan, et al., In-vitro antibacterial activities of cefpiramide and other broad-spectrum antibiotics against 440 clinical isolates in China, J. Infect. Chemother. 6 (2000) 81–85.

[34] Y. Qu, G. Noe, A.R. Breaud, M. Vidal, W.A. Clarke, N. Zahr, et al., Development and validation of a clinical HPLC method for the quantification of hydroxychloroquine and its metabolites in whole blood, Future science OA (2015) 1.

[35] Ishide T. Denopamine, A selective 1-receptor agonist and a new coronary vasodilator, Curr. Med. Res. Opin. 18 (2002) 407–413.

[36] E. Brendel, W. Wingender, Clinical pharmacology of glucosidase inhibitors, Oral Antidiabetics: Springer (1996) 611–632.

[37] R.H. Liss, M.C. Charest, J. Mead, Comparative ultrastructure of submaxillary salivary glands from mice treated with cytosine arabinoside, cyclocytidine, and anhydro-ara-5-fluorocytidine, Canc. Treat Rep. 60 (1976) 881–888.

[38] Organization Wh, International nonproprietary names for pharmaceutical substances (INN): recommended INN: list 69, WHO Drug Inf. 27 (2013) 41–93.

[39] B. Li, X. Wang, B. Rutz, R. Wang, A. Tamalunas, F. Strittmatter, et al., The STK16 inhibitor STK16-IN-1 inhibits non-adrenergic and non-neurogenic smooth muscle contractions in the human prostate and the human male detrusor, N. Schmied. Arch. Pharmacol. (2019) 1–14.

[40] C. Parker, R. Waters, C. Leighton, J. Hancock, R. Sutton, A.V. Moorman, et al., Effect of mitoxantrone on outcome of children with first relapse of acute lymphoblastic leukaemia (ALL R3): an open-label randomised trial, Lancet 376 (2010) 2009–2017.

[41] C. Kennedy, K. Gill, P. Walsh, The effects of nifurpirinol treatment on the activities of hepatic xenobiotic transforming enzymes in the gulf toadfish, Opsanus beta (Goode and Bean), J. Fish. Dis. 13 (1990) 525–529.

[42] A.G. Malykh, M.R. Sadaie, Piracetam and piracetam-like drugs, Drugs 70 (2010) 287–312.

[43] S.L. Berg, F.M. Balis, K.S. Godwin, D.G. Poplack, Pharmacokinetics, cerebrospinal fluid penetration, and metabolism of piroxantrone in the Rhesus monkey, Invest. N. Drugs 11 (1993) 255–261.

[44] J.E. Frampton, Stiripentol: a review in dravet syndrome, Drugs 79 (2019) 1785–1796.

[45] E.J. Sybertz, T. Baum, K.K. Pula, S. Nelson, E. Eynon, C. Sabin, Studies on the mechanism of the acute antihypertensive and vasodilator actions of several β-adrenoceptor antagonists, J. Cardiovasc. Pharmacol. 4 (1982) 749–758.

[46] F. Leteurtre, G. Kohlhagen, K.D. Paull, Y. Pommier, Topoisomerase II inhibition and cytotoxicity of the anthrapyrazoles DuP 937 and DuP 941 (Losoxantrone) in the National Cancer Institute preclinical antitumor drug discovery screen, J. Natl. Cancer Inst.: Journal of the National Cancer Institute 86 (1994) 1239–1244.

[47] W.E. Rose, M.J. Rybak, Tigecycline: first of a new class of antimicrobial agents, Pharmacotherapy 26 (2006) 1099–1110.

[48] K. Kageyama, T. Mizobe, S. Nozuchi, N. Hiramatsu, Y. Nakajima, H. Aoki, Toborinone and olprinone, phosphodiesterase III inhibitors, inhibit human platelet aggregation due to the inhibition of both calcium release from intracellular stores and calcium entry, J. Anesth. 18 (2004) 107–112.

[49] H. Marlow, Xamoterol, a beta 1-adrenoceptor partial agonist: review of the clinical efficacy in heart failure, Br. J. Clin. Pharmacol. 28 (1989) 23S–30S.

[50] D.E. Pires, T.L. Blundell, D.B. Ascher, pkCSM: predicting small-molecule pharmacokinetic and toxicity properties using graph-based signatures, J. Med. Chem. 58 (2015) 4066–4072.

[51] N. Baildya, N.N. Ghosh, A.P. Chattopadhyay, Inhibitory capacity of Chloroquine against SARS-COV-2 by effective binding with Angiotensin converting enzyme-2 receptor: An insight from molecular docking and MD-simulation studies, J. Mol. Struct. 1230 (2021), https://doi.org/10.1016/j.molstruc.2021.129891.